

12. INTERSTITIAL-WATER CHEMISTRY, LEG 105 SITES 645, 646, AND 647, BAFFIN BAY AND LABRADOR SEA¹

J. C. Zachos^{2,3} and T. Cederberg⁴

ABSTRACT

More than 100 interstitial-water samples from Sites 645, 646, and 647 were analyzed for major and minor ion chemistry. All sites display increases in calcium and decreases in magnesium with depth. The rate of change for these ions varies from site to site as a result of differences in rates of diffusion and sediment/water chemical reactions related to sediment lithology, physical properties, and redox conditions. The latter condition is reflected by the rate of sulfate reduction at each site. The lowest sulfate concentrations were observed at Site 645, where anomalously large depletions of calcium and magnesium are also recorded just below the sediment/water interface. Other dissolved ions, such as potassium, lithium, and strontium, also display overall anomalous depletions at Site 645. In contrast, concentration gradients of most cations at Sites 646 and 647, where dissolved sulfate is present, are more linear and may be primarily supported by diffusion between layer II basalts below and seawater above.

Interstitial-water δD and $\delta^{18}O$ display concomitant decreases with depth at each site. A minor exception occurs at Site 645, where $\delta^{18}O$ values become more positive in deeper portions of the sequence. This, together with the fact that correlations between δD and $\delta^{18}O$ vary from site to site, suggests that these isotopes are dissimilarly affected by reactions involving interstitial waters and layer II basalt and/or sediments. Interstitial-water $\delta^{18}O$ may be more sensitive to low-temperature reactions with basalts and volcanoclastics, which results in an overall depletion. Sediment diagenesis at deeper depths may slightly enrich interstitial-water $\delta^{18}O$. The effects of such processes on δD values may be negligible.

INTRODUCTION

In reconstructing paleoenvironments, scientists have become increasingly dependent on information derived from geochemical analyses of deep-sea sediments. Unfortunately, the measured chemical compositions of the biogenic and detrital components of buried sediments may not reflect their original compositions. Consequently, investigations of processes that can alter the physical and chemical characteristics of sediments have grown in importance. Interstitial-water chemistry is one method that has proved useful for identifying zones of sediment diagenetic reactions. This is primarily because small chemical changes in the sediments usually produce large changes in interstitial-water chemistry (e.g., Gieskes, 1983). For this and other reasons, such studies have now become a routine and vital portion of DSDP and ODP investigations.

During Leg 105 of the Ocean Drilling Program, Sites 645, 646, and 647 were drilled in a north-south transect from Baffin Bay to Labrador Sea. The principal objective of this leg was to gain a better understanding of the evolution of regional Cenozoic climate, ecology, and patterns of surface and deep-water circulation. The entire region experienced higher rates of sedimentation during the Neogene glaciations, although the rates and modes of sedimentation varied considerably between Baffin Bay and Labrador Sea.

The pore-water systems of hemipelagic and pelagic sequences, characterized by high sedimentation rates, usually experience reducing conditions that in turn lead to an interesting variety of chemical reactions between the more unstable sediments and in-

terstitial water. Our main purpose here is to present the results of shipboard and land-based analyses of interstitial waters collected during Leg 105 and to explore briefly the various physical and chemical processes that may influence interstitial-water chemistry.

METHODS

All samples were obtained by squeezing of 25-cm-long whole-round core sections at room temperature using a Manheim squeezer, as described by Manheim and Sayles (1974). The volume of water recovered from each sample decreased steadily with depth and ranged from 50 mL in shallow cores to less than 5–10 mL in samples from deeper cores.

Immediately following recovery, alkalinity, pH, chlorinity, salinity, and calcium and magnesium concentrations were determined using methods outlined by Gieskes (1974). Sulfate analyses were conducted at a later time by ion chromatography. IAPSO standards were used for all shipboard analyses. For later shore-based analyses, a 10-mL portion of each sample was split; one-half was poisoned with $HgCl_2$ and stored in polyethylene tubes, while the remaining one-half was acidified and stored in borosilicate glass ampules. An additional 5 mL of untreated interstitial water intended for isotope analyses was stored in glass vials.

Silicate concentrations in poisoned samples were determined by colorimetric techniques (Fanning and Pilson, 1973) and a Beckman 25 spectrophotometer. From the same samples, phosphate concentrations were determined by an auto analyzer apparatus (Lambert and Oviatt, 1986). Standard deviations were 1% for silica and 2.5% for phosphate. Dissolved strontium, potassium, and lithium values were obtained from the acidified samples by flame atomic absorption spectrophotometry. Oxygen isotopes were determined by experimental procedures similar to those of Epstein and Mayeda (1953). Deuterium abundances were determined using methods outlined by Friedman (1953) and Craig (1961). All oxygen and hydrogen isotope data are reported in the $\delta(\text{‰})$ notation relative to the standard mean ocean water (SMOW) standard (Table 1).

SITE LOCATIONS AND DESCRIPTIONS

Site 645, located at a depth of 2000 m in Baffin Bay (Fig. 1), consists of rapidly deposited hemipelagic sediments of late Miocene to Holocene age. Sedimentation at this location was strongly influenced by terrigenous influx from proximal land areas to the east, west, and north. The majority of the sediments were delivered during the Neogene glaciations at a rate exceeding 134 m/

¹ Srivastava, S. P., Arthur, M., Clement, B., et al., 1989. *Proc. ODP, Sci. Results*, 105: College Station, TX (Ocean Drilling Program).

² Graduate School of Oceanography, University of Rhode Island, Narragansett, RI 02882.

³ Now at Dept. of Geological Sciences, Univ. of Michigan, C.C. Little Bldg., Ann Arbor, MI 48109-1063.

⁴ Geologisk Centralinstitut, Kobenhavns Universitet, Oster Voldgade 10, DK-1350 Kobenhavn K, Denmark.

Table 1. Alkalinity, pH, salinity, major and minor ions, and nutrient concentrations, and stable oxygen and deuterium isotope compositions of interstitial-water samples from Sites 645, 646, and 647.

Core, section, interval (cm)	Depth (mbsf)	pH	Alkalinity (meq/L)	Salinity (‰)	Chlorine (‰)	Calcium (mmol)	Magnesium (mmol)	Sulfate (mmol)	δD (SMOW)	$\delta^{18}O$ (SMOW)	Silica (μ mol)	Phosphate (μ mol)	Strontium (μ mol)	Lithium (μ mol)	Potassium (mmol)	Magnesium (μ mol)
112-645B-1H-2, 140-150	2.9	7.81	3.99	34.0	19.47	10.08	49.54	21.9	-2.6	-0.74	146	3.8	78	41	10.3	39.0
645B-5-2, 140-150	35.1	7.90	4.71	30.1	18.66	4.41	32.35	0.6	-0.6	-0.31	160	7.6	87	32	7.5	8.6
645B-9-2, 140-150	74.5	7.83	4.36	30.0	17.79	5.65	33.06	3.1	-4.4	-0.89	134	—	78	36	5.1	8.6
645B-11-2, 140-150	93.8	7.94	4.80	31.0	19.34	5.45	31.54	0.9	-4.1	-0.81	—	3.4	63	34	3.4	3.1
645B-14-3, 140-150	124.3	8.05	4.51	30.8	19.00	5.29	32.56	1.3	-4.8	-0.93	—	—	74	36	2.9	3.1
645B-19-3, 140-150	172.5	7.99	5.11	31.6	19.63	4.94	32.52	1.8	-7.2	-1.45	—	—	58	40	3.2	3.2
645B-21-5, 140-150	194.8	7.93	5.99	31.0	17.51	4.71	34.31	2.2	-8.3	-1.48	199	—	—	—	—	—
645B-24-5, 140-150	223.6	7.93	12.13	32.0	19.85	4.61	32.53	1.2	-6.8	-1.56	543	10.0	70	53	4.2	4.5
645B-27-3, 140-150	249.6	7.96	9.26	30.1	18.46	6.31	32.95	9.3	-11.3	-1.90	361	—	—	—	—	—
645B-30-6, 140-150	283.1	8.07	12.88	29.9	17.12	6.14	28.05	1.7	-7.1	-1.56	490	13.7	33	48	3.4	3.6
645D-1-3, 140-150	269.8	8.00	12.38	32.5	19.09	7.06	33.71	6.0	-10.9	-1.94	311	10.9	58	45	4.2	5.0
645D-8-2, 140-150	304.7	7.94	16.48	25.0	20.67	7.88	29.54	1.4	-10.6	—	616	17.6	52	57	3.4	5.0
645D-11-5, 140-150	376.8	8.05	13.50	30.5	18.09	7.48	26.90	2.3	-10.9	-2.22	507	—	60	56	3.3	4.3
645D-14-3, 140-150	402.7	8.01	12.29	30.0	19.92	7.51	28.19	3.5	-11.9	-2.43	—	—	71	60	3.3	3.2
645D-17-4, 140-150	433.1	8.16	12.52	32.1	19.70	7.59	27.57	2.8	-11.8	-2.47	—	—	—	—	—	—
645D-20-3, 140-150	460.6	8.21	13.81	31.0	19.11	8.03	26.66	1.5	-12.2	-2.48	—	—	90	81	3.2	3.6
645E-4-3, 140-150	459.6	8.01	11.11	32.5	19.33	7.73	26.91	3.2	-11.8	-2.49	136	4.7	—	—	—	—
645E-7-4, 140-150	490.0	7.80	13.57	31.9	18.55	8.42	25.83	3.4	-11.9	-2.77	663	12.7	66	103	3.8	10.9
645E-10-2, 140-150	515.9	7.85	13.66	31.9	19.65	9.13	24.03	2.5	-12.5	-2.98	544	9.1	—	—	—	—
645E-13-5, 140-150	549.2	—	—	31.0	19.45	9.69	20.52	3.0	—	—	—	8.1	74	90	3.2	5.1
645E-16-4, 140-150	576.7	7.91	8.02	31.5	19.12	10.27	24.68	4.1	-12.8	-2.86	—	—	—	—	—	—
645E-19-4, 140-150	605.7	7.91	8.02	31.4	18.51	10.51	24.75	5.5	-13.8	-2.83	143	1.7	98	80	3.4	8.0
645E-23-2, 140-150	631.3	8.13	6.62	31.0	19.28	10.73	22.28	6.7	-14.7	-2.74	91	1.1	109	86	3.7	6.5
645E-26-2, 140-150	660.0	8.20	6.66	30.5	18.69	11.97	21.27	3.2	-13.3	-2.70	129	1.3	—	—	—	—
645E-29-5, 140-150	693.4	7.92	7.66	30.5	18.65	12.95	18.79	3.7	-14.3	-2.81	607	—	—	—	—	—
645E-33-3, 140-150	719.1	—	—	30.0	18.67	14.93	20.72	3.7	-14.6	-2.83	—	—	—	—	—	—
645E-36-1, 140-150	745.1	7.96	12.66	31.5	17.67	13.86	18.29	2.7	-14.9	-2.69	—	9.0	—	—	—	—
645E-39-4, 140-150	778.6	8.24	12.77	30.2	18.37	14.15	18.24	4.9	-16.3	-2.55	—	—	—	—	—	—
645E-43-5, 140-150	818.6	—	—	30.5	17.97	18.06	15.65	7.6	—	—	—	—	—	—	—	—
645E-46-3, 140-150	844.5	—	—	30.4	19.47	17.24	15.48	4.0	—	—	—	6.4	—	—	—	—
645E-49-5, 140-150	876.0	—	—	32.1	18.79	15.24	15.83	4.0	—	—	—	—	—	—	—	—
645E-53-5, 140-150	905.0	—	—	30.5	18.79	14.20	17.41	4.6	—	—	—	—	—	—	—	—
645E-56-4, 140-150	932.6	—	—	30.7	18.92	15.80	16.04	5.1	—	—	—	—	—	—	—	—
645E-59-5, 140-150	963.0	—	—	30.0	17.84	17.73	15.66	6.4	—	—	—	7.4	—	—	—	—
645E-62-5, 140-150	991.6	—	—	33.0	21.37	18.14	16.34	8.4	—	—	—	—	—	—	—	—
645E-65-5, 140-150	1021.0	—	—	29.0	19.68	16.38	13.60	3.5	—	—	—	—	114	898	3.45	8.0
645E-68-5, 140-150	1050.0	—	—	29.0	17.60	16.89	15.73	6.4	—	—	—	—	—	—	—	—
645E-69-5, 140-150	1059.6	—	—	28.0	17.05	17.43	14.02	6.9	—	—	—	5.6	—	—	—	—
645E-75-3, 140-150	1113.7	—	—	29.0	16.67	15.66	14.24	3.9	—	—	—	—	—	—	—	—
645E-78-4, 140-150	1143.7	—	—	27.9	16.97	14.93	13.03	3.9	—	—	—	7.1	—	—	—	—
646A-1-3, 140-150	4.4	8.01	5.84	34.8	20.06	9.79	49.78	22.5	2.3	0.34	—	—	93	35	—	101
646B-2-4, 140-150	9.8	7.99	5.72	34.4	19.70	9.81	49.37	20.7	3.0	0.30	526	—	78	29	9.9	79
646A-4-5, 140-150	33.6	8.38	5.58	33.9	19.76	9.19	44.17	15.8	2.9	0.12	—	—	82	29	10.0	35
646B-5-2, 140-150	39.8	8.17	5.23	33.9	19.77	8.88	44.71	14.0	3.0	0.12	472	11.8	81	29	10.4	27
646A-7-4, 140-150	61.0	7.80	3.82	32.7	19.52	9.49	38.82	10.1	1.9	-0.18	—	—	84	28	9.5	15
646B-9-5, 140-150	79.8	8.14	4.89	33.5	20.32	10.46	38.32	7.8	2.7	-0.19	472	8.3	82	29	9.2	22
646A-10-4, 140-150	90.0	8.23	5.06	32.7	19.38	11.17	35.59	6.4	1.3	-0.43	—	—	82	31	8.4	25
646B-12-4, 140-150	107.3	8.27	4.83	32.5	19.56	11.47	34.74	5.5	1.5	-0.58	513	7.9	98	37	7.6	30
646B-18-2, 140-150	162.0	7.98	3.89	32.0	20.14	12.32	31.87	1.8	-0.3	-0.88	451	7.7	98	40	7.5	19
646B-21-4, 140-150	194.1	7.78	4.31	32.0	20.03	15.11	30.63	2.5	-0.8	-1.02	381	5.7	93	47	7.4	20
646B-26-4, 140-150	242.0	7.60	2.97	32.5	20.27	20.66	27.81	1.0	-1.5	-1.51	606	8.8	101	60	6.2	14
646B-30-4, 140-150	280.9	7.32	2.86	32.2	20.11	28.43	22.20	1.2	-2.2	—	525	8.2	78	66	5.0	22
646B-33-4, 140-150	310.0	7.73	1.52	32.3	20.18	34.51	17.99	0.5	-2.7	-2.01	355	5.9	67	78	3.8	25
646B-37-5, 140-150	350.2	7.94	0.81	32.5	20.18	46.29	11.94	1.8	-3.3	-2.16	155	2.9	78	79	2.0	19
646B-40-5, 140-150	379.1	7.98	0.69	33.0	20.11	49.60	10.21	1.7	-3.9	-2.34	155	2.4	68	82	1.8	17

646B-43-2, 140-150	403.6	7.95	0.76	33.0	19.94	54.46	9.85	2.0	-4.4	-2.37	165	2.9	68	84	1.1	22
646B-50-1, 140-150	469.6	7.84	0.48	33.7	19.44	57.88	10.62	7.0	-4.5	-2.11	203	2.3	59	87	1.0	32
646B-55-1, 140-150	517.9	7.41	0.44	33.7	20.09	60.45	9.53	2.5	-5.7	-2.65	143	2.1	55	88	1.3	42
646B-58-2, 140-150	548.4	7.85	1.10	34.1	19.88	55.77	13.59	7.1	-4.4	-2.09	124	2.3	67	91	1.3	58
646B-61-1, 140-150	575.4	8.08	1.15	33.0	19.74	56.60	13.54	7.8	-4.4	-2.33	115	2.4	62	94	1.1	58
646B-65-3, 140-150	616.9	7.97	1.18	33.5	19.81	61.88	6.08	3.4	-6.3	-3.20	177	2.5	74	114	1.0	37
646B-68-3, 140-150	645.7	7.84	0.92	34.0	20.27	59.53	9.98	4.8	-6.2	-2.88	139	2.1	95	118	1.2	60
646B-72-2, 140-150	682.7	7.83	0.51	32.8	19.80	58.24	7.78	5.5	-6.8	-2.84	113	1.8	147	130	1.2	45
646B-75-4, 140-150	714.5	8.23	0.97	32.3	19.58	58.72	7.06	4.4	—	—	—	4.0	—	—	—	—
646B-79-1, 140-150	748.8	8.11	0.79	32.5	19.59	59.70	7.56	4.1	-7.4	-3.11	—	—	236	140	1.2	53
647A-1-5, 140-150	7.4	7.45	2.30	34.5	19.13	10.79	50.18	26.6	1.3	0.27	294	12.5	79	36	10.7	—
647A-6-5, 140-150	56.0	7.66	2.18	34.2	19.70	12.81	46.06	21.1	2.2	-0.17	131	2.9	109	36	7.9	—
647A-9-3, 140-150	82.0	7.67	2.43	34.2	19.97	14.08	43.47	22.1	0.6	-0.50	140	3.6	123	48	7.6	—
647A-12-3, 140-150	111.1	7.57	4.01	34.0	19.68	15.36	43.28	21.3	-0.5	-0.76	248	4.4	133	72	7.7	—
647A-15-2, 140-150	138.3	7.51	3.35	33.9	19.34	16.11	45.41	23.4	-0.9	-0.75	556	8.7	128	72	9.0	—
647A-19-5, 140-150	181.2	6.20	3.03	34.1	19.63	19.47	41.96	23.0	-1.8	-1.76	899	12.3	166	115	8.5	—
647A-23-2, 140-150	215.2	7.15	4.82	34.4	19.70	22.37	41.32	22.4	-2.7	-2.10	679	10.9	189	133	8.2	—
647A-27-5, 140-150	257.8	7.57	2.65	34.0	19.86	19.26	42.24	23.3	-1.5	-0.60	346	5.3	139	81	9.6	—
647A-30-5, 140-150	286.8	6.98	3.11	33.9	19.20	26.40	38.45	20.8	-4.4	-2.75	328	4.5	228	171	6.1	—
647A-36-3, 140-150	341.6	—	—	33.0	18.79	29.15	33.29	19.3	-5.2	-2.76	—	3.8	—	—	—	—
647A-39-2, 140-150	369.0	—	—	33.1	19.16	31.64	32.04	17.1	-5.6	-3.36	—	4.2	—	—	—	—
647A-42-5, 140-150	402.5	—	—	33.1	19.38	32.86	26.47	15.9	-3.0	-1.30	103	2.1	296	248	4.6	—
647A-45-4, 140-150	430.0	7.38	1.74	33.7	19.17	24.77	37.44	20.5	-5.9	-3.16	66	1.4	195	146	6.5	—
647A-48-5, 140-150	460.6	7.58	1.67	34.1	19.05	36.12	28.65	17.2	—	—	—	2.8	291	269	4.1	—
647A-51-5, 140-150	489.5	—	—	33.0	18.88	34.50	28.10	13.2	—	—	—	—	—	—	—	—
647A-54-4, 140-150	517.0	—	—	32.5	19.13	38.53	28.42	14.3	—	—	191	2.5	—	—	—	—
647A-64-2, 140-150	620.4	—	—	33.8	19.27	47.11	27.06	15.7	—	—	128	1.9	—	—	—	—
647A-67-2, 140-150	649.4	—	—	33.1	18.60	43.88	28.86	15.9	—	—	—	3.6	—	—	—	—

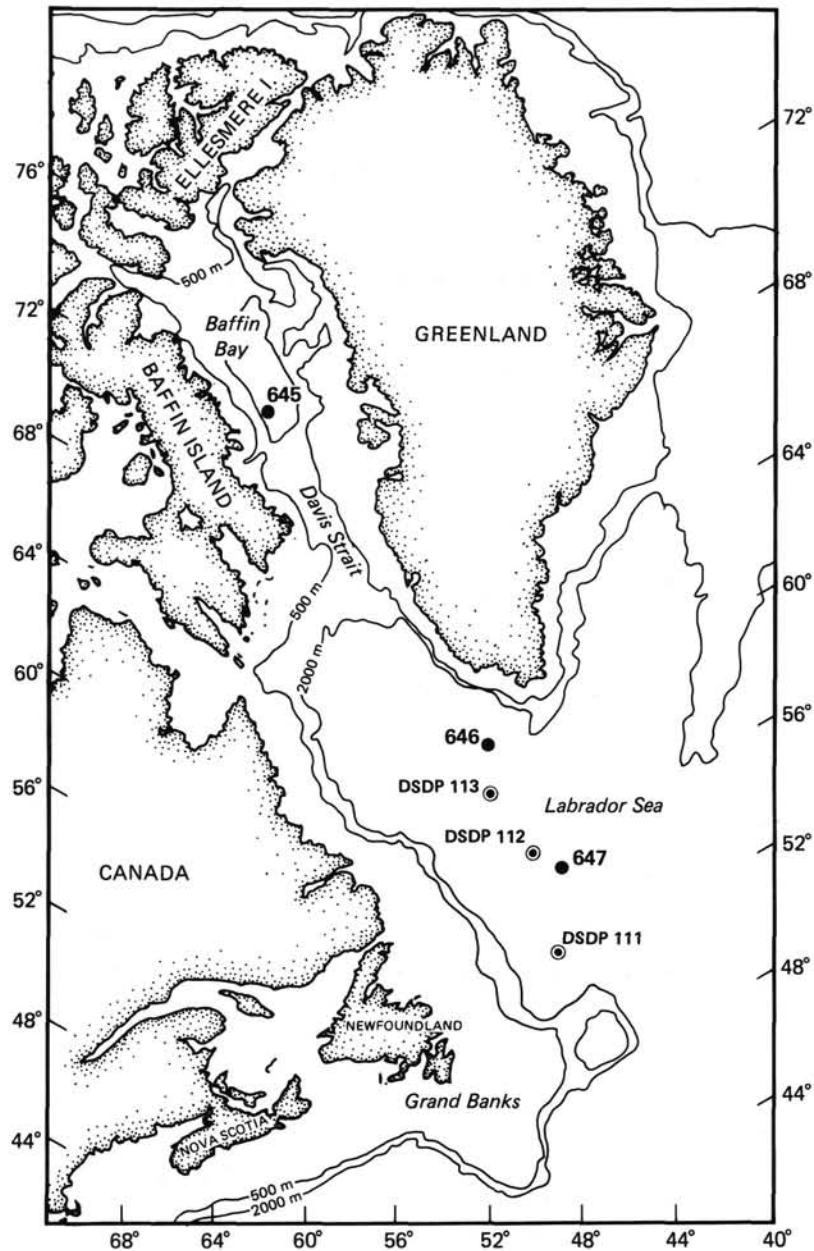


Figure 1. Locations of the Leg 105 sites in Baffin Bay and Labrador Sea.

m.y. The sedimentary section at Site 645 was divided into three distinct lithologic units. Unit I (0–168 mbsf) consists mainly of calcareous and gravel-bearing muddy sands, calcareous silty muds, and silty clays. The average carbonate content is about 30%. This unit, as well as underlying units, contains large concentrations of pyrite. Unit II (168–320.4 mbsf) contains slightly less carbonate but is still dominated by cobble-bearing silt and clay sediments. Unit III (340–1147 mbsf) lacks the dropstones common in the upper units. The major lithologies are represented by homogeneous, poorly sorted muddy sands and sandy silty muds having less than 5% carbonate. This unit is composed of several subunits; however, the boundaries between these subunits are somewhat arbitrary and as such are unimportant to this discussion.

Site 646, located in the Labrador Sea (Fig. 1), was drilled on the western edge of the Eirik Ridge, a large east/west-trending sediment drift, in 3460 m of water. The sediments here consist

of late Miocene to late Pliocene calcareous silty clays and claystones overlain by low-carbonate silty clays of Pliocene to Holocene age. Sedimentation rates at this site generally exceed 90 m/m.y. The sequence was divided into two distinct units. Unit I (0–236 mbsf) is composed of silty clay, clayey silt, and clay with assorted ice-rafted debris, with a biogenic component that is a mixture of both opaline and calcareous microfossils. Unit II (236–766 mbsf) has a similar major lithology but is somewhat more homogeneous and fine-grained and contains only a calcareous biogenic component.

The final site of the transect, Site 647, is located in the southern Labrador Sea at a water depth of 3870 m (Fig. 1). This site received less terrigenous material than the other locations, and as a result biogenic materials constitute a higher percentage of the total sediment. Site 647 was the only site from Leg 105 at which basement was penetrated, with the recovery of 37 m of basalt below 699 mbsf. The sedimentary sequence here was di-

vided into four lithologic units. Unit I (0–116 mbsf) is represented by interbedded silty clays, clayey muds, and clayey silts, with variable amounts of biogenic components and gravel. Unit II (116–135.4 mbsf), a condensed unit, has a slightly variable lithology of silty and nanofossil clay, the upper portion of which contains abundant numbers of calcareous nanofossils. The lower portion is depleted in calcareous nanofossils but does contain up to 15% biosiliceous material. Unit III (135–530 mbsf) has been subdivided into several subunits, each of which consists of claystone and clayey ooze, with a high biogenic carbonate component (25%–50%). Biosiliceous material is abundant over a short interval from 212 to 241 mbsf, where the sediments contain a greater than 60% siliceous component. Unit IV (530–699 mbsf) has essentially the same major lithology as the overlying unit, but contains less biogenic material. In addition, the sediments in the lower part of this unit, just above the basement basalts, bear a red hue as a result of iron-oxide coatings. Dolomite and siderite concretions and scattered chert and gypsum crystals were also observed in this unit.

RESULTS

Site 645

The most striking feature of the chemical profiles from Site 645 is the rapid decrease in sulfate concentrations over the upper 25 m (Fig. 2). Sulfate concentrations decrease from 22 mmol to less than 1 mmol over this interval, most likely, as a result of sulfate reduction processes. This is a characteristic phenomenon of hemipelagic sites with high sedimentation rates. A slight peak in the sulfate profile occurs at 250 mbsf, within a sandy layer in which recovery was poor. Farther downhole, sulfate increases slightly by several millimols, indicating a possible source of sulfate from below.

A by-product of the sulfate reduction reaction is bicarbonate ion. At Site 645, alkalinity values are low through Unit I, the zone of maximum sulfate reduction, and then increase rapidly below, reaching a peak at about 250 mbsf (Fig. 2). Inspection of the calcium and magnesium profiles reveals that the concentrations of both ions decrease sharply in Unit I. Calcium is depleted by 4 to 5 mmol, while magnesium decreases by 16 to 18 mmol over the upper 25 m of the section.

Salinity and chlorinity concentrations also display considerable variability at this site. In less than 20 m below the sediment/water interface, salinity values decrease by nearly 4‰. A substantial portion of this decrease can be attributed to the loss of sulfate ions and, to a lesser extent, to the decreases in magnesium and calcium over the same interval. Slightly larger salinity variations were observed farther downhole. Originally, we thought that these variations might represent dilution by freshwaters of either glacial or gas hydrate origin. However, neither idea is well supported by other evidence (i.e., oxygen and hydrogen isotopes). Possibly, the anomalous value recorded at 304.7 mbsf resulted from contamination during sampling.

Potassium, strontium, and lithium were determined on a small number of samples over the interval 0 to 650 mbsf and on a single sample from 1030 mbsf (Fig. 2). Potassium concentrations decrease rapidly from seawater values over the upper 100 m and then remain more or less constant from that point down. With the exception of a single sample from the lower portion of the hole that yielded a value of $>800 \mu\text{mol}$, lithium contents also show little change with depth, increasing slightly downhole by $50 \mu\text{mol/L}$. Strontium concentrations are also low, averaging less than $80 \mu\text{mol}$ over the length of the hole.

Stable oxygen and hydrogen isotope analyses were conducted on samples from the top of Hole 645 to 800 mbsf. δD values display a gradual depletion with depth, decreasing from -2.6‰ at the sediment/water interface to -16.3‰ at 778 mbsf (Fig. 2).

The rate of decrease is most rapid over the upper several hundred meters. Although $\delta^{18}\text{O}$ values show a similar pattern over the upper portion of the sequence, decreasing from -0.74‰ near the sediment/water interface to -2.98‰ at 515 mbsf, values actually increase slightly in the lower portions of the sequence, reaching -2.55‰ at 778 mbsf.

A limited number of dissolved silica and phosphate analyses produced somewhat erratic results. Silica concentrations were found to be less than $200 \mu\text{mol/L}$ through Unit I, the interval of high carbonate concentrations. This is in contrast to the silica trends seen in lithologic Units II and III, which show large-magnitude variations with values as high as $700 \mu\text{mol/L}$ and as low as $100 \mu\text{mol/L}$.

Site 646

As at Site 645, sulfate concentrations decrease with depth at Site 646 (Fig. 3). However, in comparison, the rate of reduction is apparently much lower at Site 646 as the most-depleted values were recorded at a depth of 180 mbsf. From this interval to 350 mbsf, concentrations average less than 2 mmol. Slightly higher values are recorded in samples from below 350 mbsf, indicating a possible source of sulfate from below.

Alkalinity values decrease almost linearly from 6 meq/L at the sediment/water interface to less than 1 meq/L at 350 mbsf. No peak in alkalinity is associated with the maximum point of sulfate reduction, indicating that the small amount of carbonate ion produced is being consumed by reactions involving authigenic minerals.

Calcium and magnesium contents display an inverse correlation with depth. The highest slopes of these concentration gradients occur over the interval of 140–350 mbsf. Below 350 mbsf, little change in the concentration of either cation can be seen.

Potassium decreases with depth as proportional to magnesium at a 1:4 molar ratio (Fig. 4). Lithium increases gradually with depth from $30 \mu\text{mol/L}$ near the top to $140 \mu\text{mol/L}$ above the base of the sequence. Strontium contents show an increase at depth but only near the bottom of the sequence.

Interstitial water δD and $\delta^{18}\text{O}$ values from just below the sediment/water interface at this site are 2.30 and 0.34‰, respectively. Below this point δD decreases to -7.4‰ at 748 mbsf. The rate of decrease above 400 mbsf is $-1.85\text{‰}/100 \text{ m}$, while below it averages -0.88‰ . A similar change in the rate of decrease is seen in the $\delta^{18}\text{O}$ compositions, which change at a rate of $-0.68\text{‰}/100 \text{ m}$ above 400 mbsf and at $-0.22\text{‰}/100 \text{ m}$ below.

The presence of biogenic siliceous material in Unit I is reflected in the interstitial-water silica concentrations, which average about $475 \mu\text{mol/L}$ throughout this unit. In contrast, silica concentrations of samples from Unit II, average about $200 \mu\text{mol/L}$. Phosphate values exhibit a similar downhole trend, decreasing from $9 \mu\text{mol/L}$ in Unit I to less than $2 \mu\text{mol/L}$ in Unit II.

Chlorinity contents remain mostly constant with depth; however, salinity decreases by 3 to 4‰ from the sediment/water interface to 200 mbsf. As at Site 645, the decrease is most likely related to the loss of sulfate ions within this interval ($30 \text{ mmol/L sulfate} = \approx 3 \text{ g/L} \rightarrow \Delta\text{S}\text{‰}$ of $\approx 3\text{‰}$).

Site 647

The concentrations of dissolved minerals at Site 647 display slightly different downhole trends in comparison with the previously discussed sites (Fig. 5). Sulfate concentrations decrease with depth, again due to the reduction processes mentioned earlier; however, the rate of reduction must be low as concentrations never fall below 12 mmol. Alkalinity values are also low, never exceeding 5 meq/L. Apparently, the lower pelagic sedimentation rates here have allowed most of the labile organic

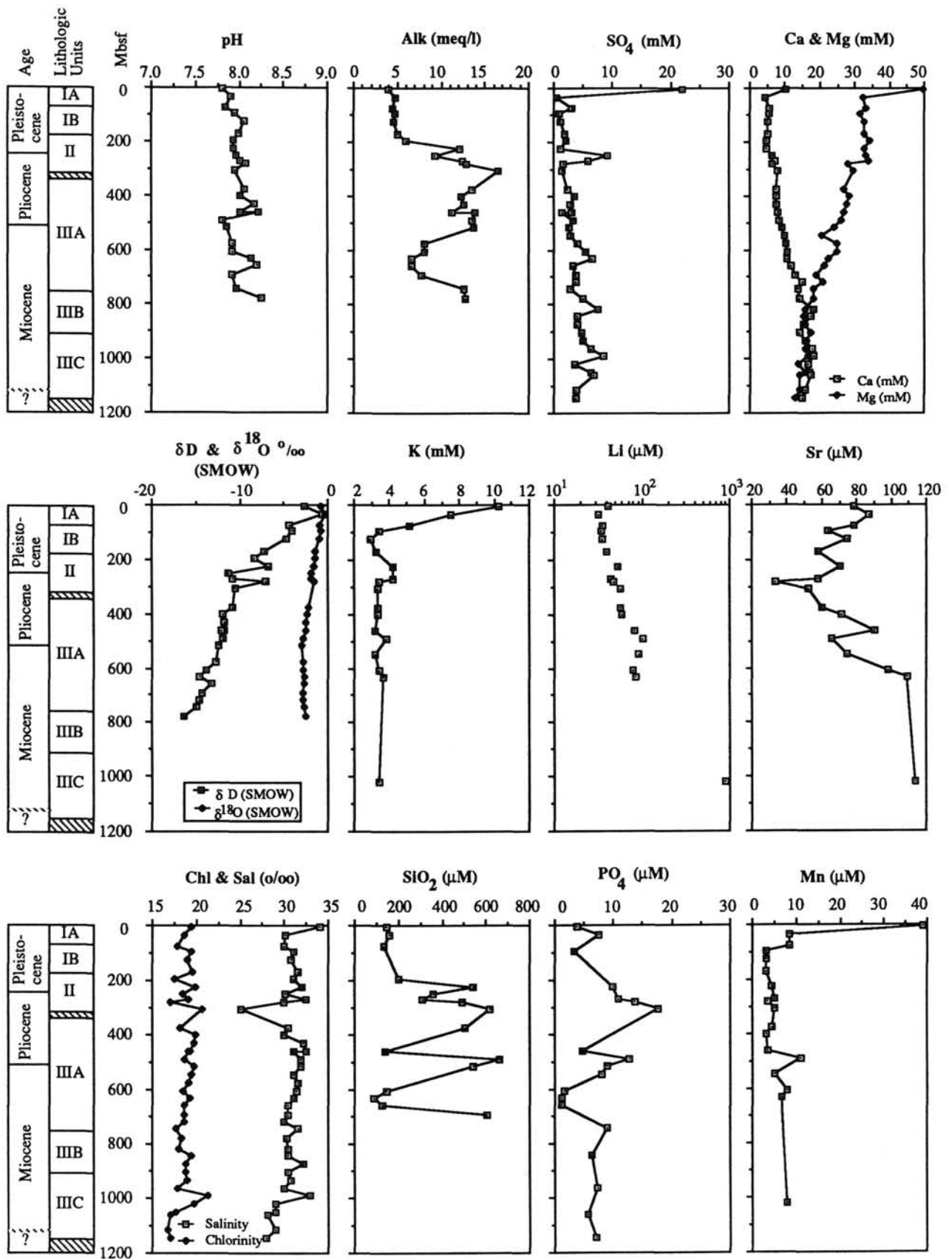


Figure 2. Plot of Site 645 interstitial-water ion concentrations and stable isotope compositions vs. depth below the sediment/water interface.

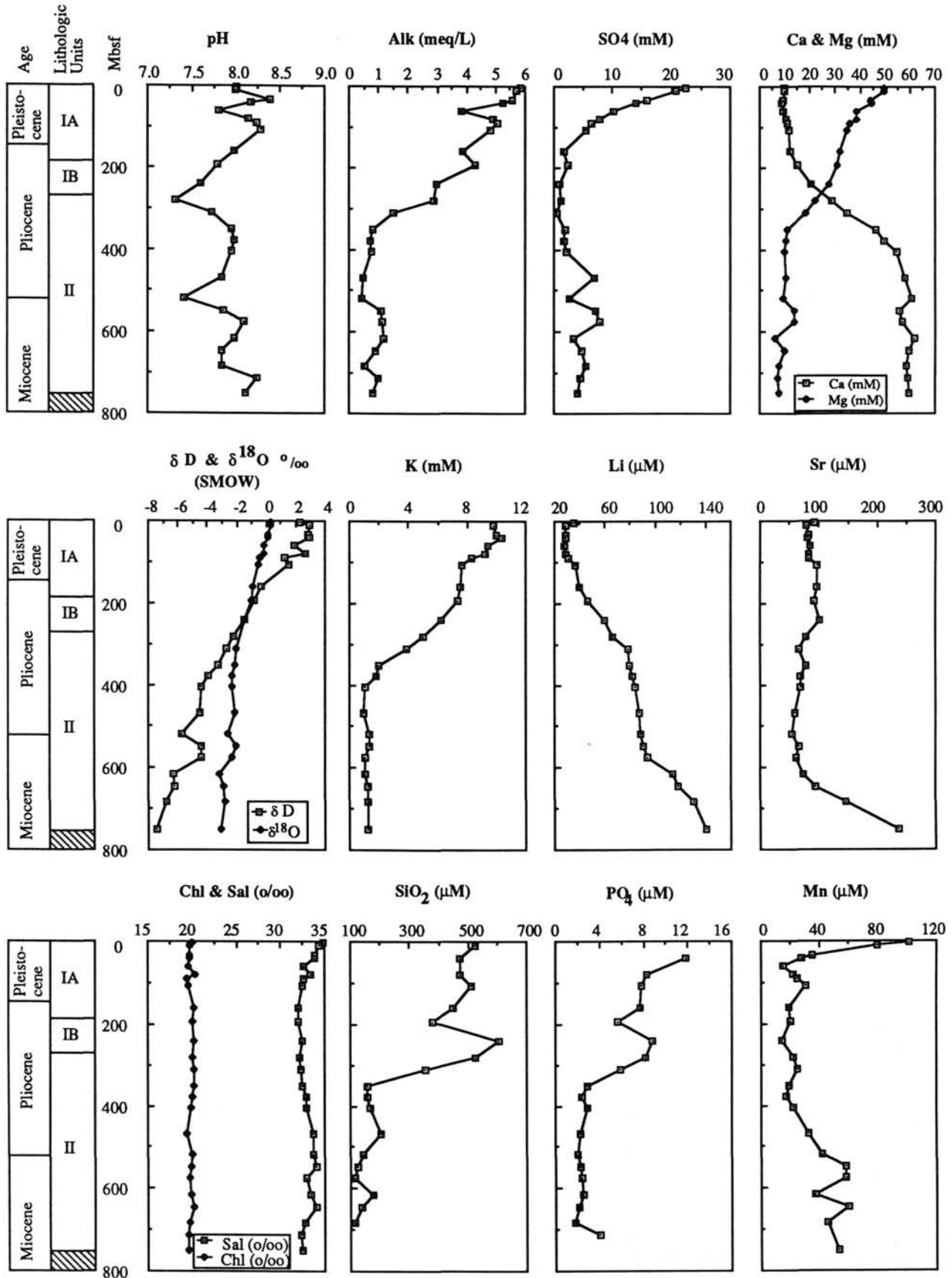


Figure 3. Plot of Site 646 interstitial-water ion concentrations and stable isotope compositions vs. depth below the sediment/water interface.

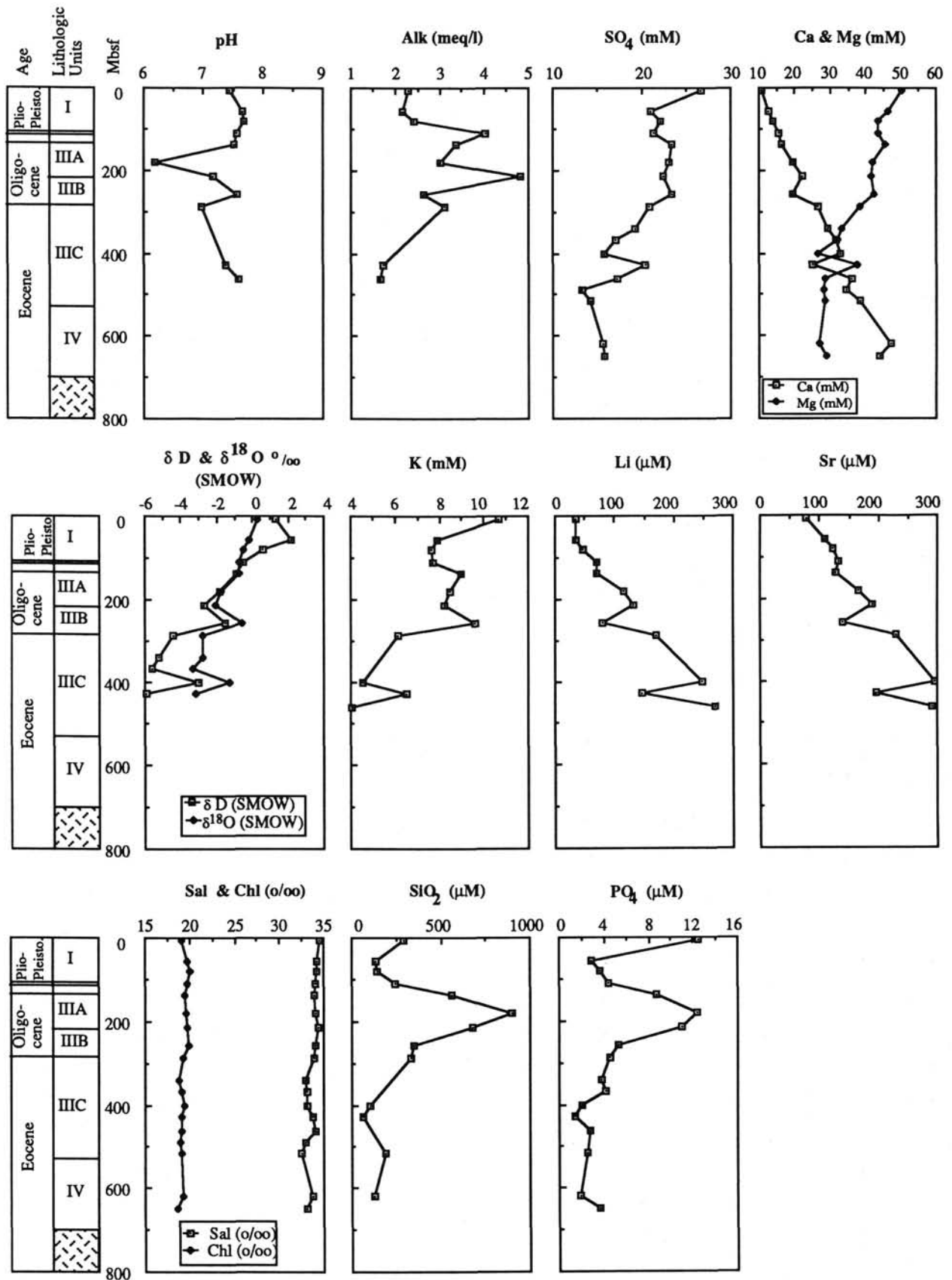


Figure 4. Plot of Site 647 interstitial-water ion concentrations and stable isotope compositions vs. depth below the sediment/water interface. Anomalous values at 257 and 430 mbsf are the result of contamination by drilling fluids.

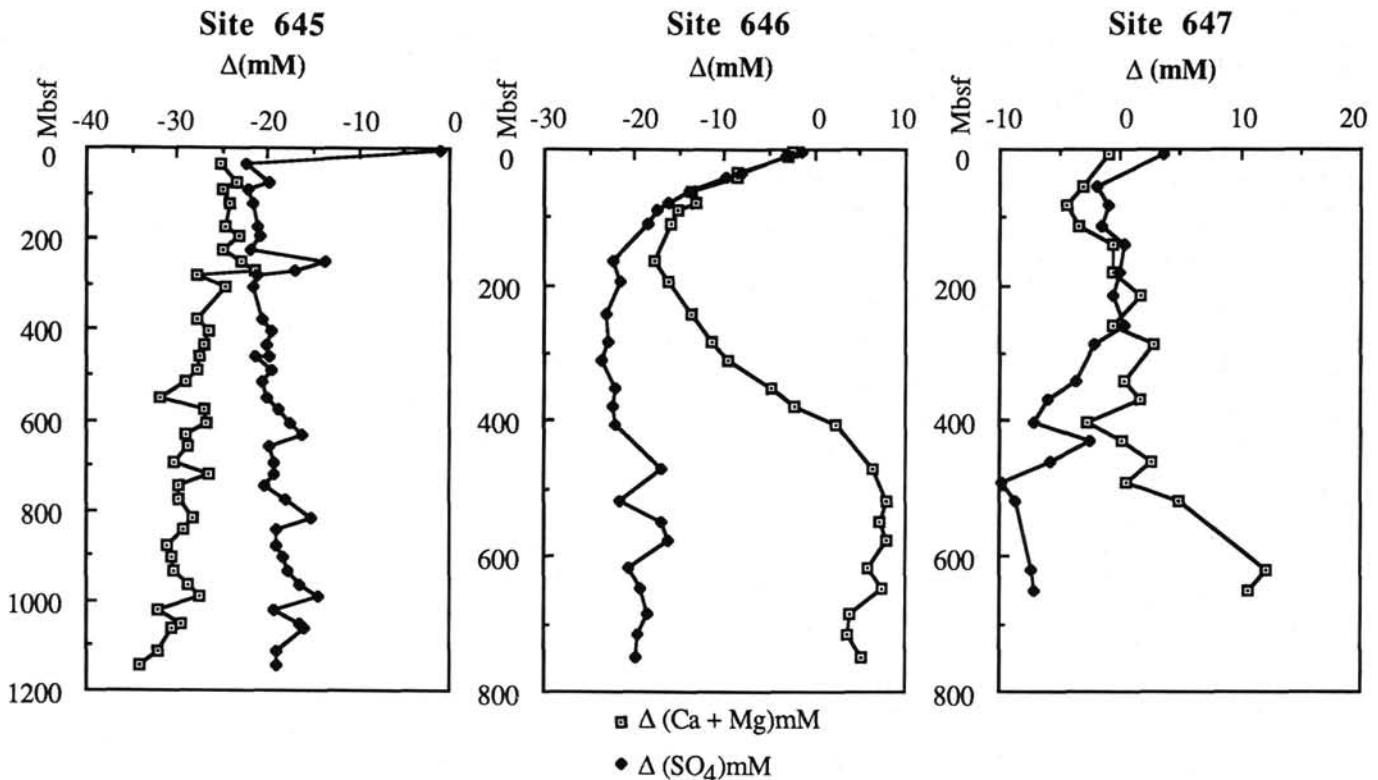


Figure 5. The change (Δ) in sulfate ion and in the combined net magnesium and calcium ion concentrations from seawater values at each site.

carbon to be consumed near the sediment/water interface before burial. Average organic carbon contents are generally less than 0.3% and exceed this value in only a few intervals.

Calcium concentrations increase approximately linearly from 10 mmol near the sediment/water interface to 38 mmol near the basement, yielding a rate of increase with depth of 5.6 mmol/100 m. This coincides with a linear decrease in magnesium concentrations of 22 mmol over the same interval. Contamination by drilling fluids (mostly surface seawater) produced the anomalous values at 257 and 430 mbsf.

Trace-element analyses were conducted on samples from the upper 480 m at this site. Both lithium and strontium concentrations increase linearly with depth at rates of 51 and 46 $\mu\text{mol}/100$ m, respectively. A fairly strong downhole correlation exists between strontium, lithium, and calcium. A general 1:4 molar relationship was observed in the rate of decrease in potassium and magnesium at this site (Fig. 4).

Similar to the trend observed at Site 646, interstitial water δD and $\delta^{18}\text{O}$ values several meters below the interface are slightly enriched relative to average seawater. From 56 to 430 mbsf, δD compositions show a gradual depletion of 7.2‰. Over the same interval, $\delta^{18}\text{O}$ decreases by 3.88‰. The rate of decrease for oxygen at Site 647 is highest among the three Leg 105 sites, averaging $-0.90\text{‰}/100$ m.

Both silica and phosphate profiles are alike, showing maxima at 190 mbsf. The interstitial-water silica contents may be sensitive to the changing concentrations of sedimentary biogenic opal, which makes up more than 60% of the total sediment in the upper portions of lithologic Unit III. The total organic carbon contents are also high ($> 1\%$) over this interval.

DISCUSSION

McDuff and Gieskes (1976) attempted to evaluate the relative importance of diffusion, advection, and sedimentary reactions

by modeling diffusion as a function of porosity, as determined from resistivity measurements. They demonstrated that the shape of observed chemical profiles could be attributed to diffusion processes alone at several pelagic DSDP sites that were either characterized by low sedimentation rates and/or located on relatively young seafloor. They suggested that the concentration gradients of calcium and magnesium ions at these sites were essentially supported by diffusion between layer II basalts and bottom waters. The principal reaction occurring in layer II is the low-temperature alteration of basalt ($< 70^\circ\text{C}$), during which calcium is leached from the basalt by hydrogen ion, and magnesium, potassium, and sodium are incorporated into alteration products, such as smectite (Seyfried and Bischoff, 1979). Mass transport by diffusion, or advection if the sediment cover is very thin, then produces the characteristic inverse gradients (Lawrence et al., 1975; McDuff, 1981) in which the increases in calcium with depth may be matched mole for mole by the decreases in magnesium, potassium, and sodium. However, deciphering the processes that maintain interstitial-water chemical gradients at pelagic and hemipelagic sites, where sedimentation rates are high, is somewhat more problematic.

At hemipelagic locations, the calcium and magnesium ion gradients often display "nonconservative" trends that vary considerably from site to site. Such differences may occur for several reasons. As sedimentation rates increase, the rate of diffusion cannot keep pace with the rapid upward migration of the sediment/water interface (Gieskes, 1974). Also, as the overburden increases, the sediments become more compacted, porosities decrease and, as a result, the rate of diffusion diminishes. Furthermore, with higher sedimentation rates, organic matter is buried more rapidly, which allows a greater percentage of reactive carbon to be preserved. With the onset of bacteria-mediated decay, the pH of interstitial water decreases, oxygen is rapidly consumed, and reduction of secondary oxidants occurs, en-

hancing sediment/interstitial-water chemical exchange reactions. As a result, "nonlinear" chemical gradients develop in the interstitial-water systems.

In general, interstitial-water calcium, lithium, and strontium increase and magnesium and potassium decrease with depth at each of the Leg 105 sites. However, the rate of change for each element varies considerably from site to site. The highest and most linear concentration gradients occur at Site 647, suggesting that the primary control on the observed gradients here may be diffusion between the calcium-enriched and magnesium-depleted formation waters of layer II basalts below and seawater above (e.g., McDuff and Gieskes, 1976). Evidence to support this comes from sediment composition studies of Nielsen et al. (this volume), which show that the transition-sediments just above the basement rocks at Site 647 are rich in authigenic, nontronitic smectite and chlorite. During the conversion of primary basement basalts and/or sedimentary volcanics to smectite, magnesium and potassium were sequestered and calcium, lithium, and strontium released from the rock (Seyfried and Bischoff, 1979; Seyfried et al., 1984; Gieskes et al., 1986). The Site 647 whole-rock sediment magnesium/aluminum and potassium/aluminum ratios also increase with depth and are higher than those ratios measured in Atlantic abyssal red clays, further confirming the authigenic origin of the smectites (Arthur et al., Nielsen et al., this volume).

The concentration gradients at Site 645 are much more subtle and nonlinear than those at Site 647. Although smectite is fairly abundant throughout Unit III (335–1147.1 mbsf), often making up more than 70% of the total sediment, most of it may be detrital rather than authigenic in origin (Thiebault et al., this volume). Thus, the relatively smaller calcium and magnesium gradients at Site 645 may reflect the minor influence of low-temperature alteration of sedimentary volcanics and/or layer II basalts on interstitial-water chemistry.

Site 646 possesses relatively high, but distinctly nonlinear, concentration gradients. We believe that here, as at Site 647, the overall diffusion gradients are supported by the low-temperature alteration of layer II basalts and/or sedimentary volcanics. Unfortunately, when this study was written, we lacked sufficient data on sediment composition to make a reasonable interpretation of the interstitial-water data.

Role of Sulphate Reduction and Authigenic Mineral Formation

Each of the Leg 105 sites is characterized by high but variable rates of sulfate reduction, the extent of which may be closely coupled to sedimentation rate. At Site 645, where Pliocene-Pleistocene sedimentation rates exceed 120 m/m.y., dissolved sulfate is essentially depleted at a depth of 35 mbsf. In contrast, at Site 647, where Pliocene-Pleistocene sedimentation rates average 44 m/m.y., sulfate is only partially depleted at depth. At Site 646, dissolved sulfate is present in interstitial waters to about 200 mbsf. Sedimentation rates at Site 646 averaged 90 m/m.y. through the Neogene and are intermediate in comparison with the rates at Sites 645 and 647 (Fig. 6). We do not mean to imply that the redox state of all deep-sea sediment/pore-water systems is simply a function of sedimentation rate alone. Other factors, such as the rain rate of organic matter, the magnitude of which often co-varies with sedimentation rates, and the oxygen content of bottom waters at the time of deposition are important as well (Emerson, 1985). However, at these and other hemipelagic sites, one can see that, for the most part, sedimentation rate dictates the rate of sulfate reduction.

The sulfate reduction reaction can be represented by this simple stoichiometric equation:

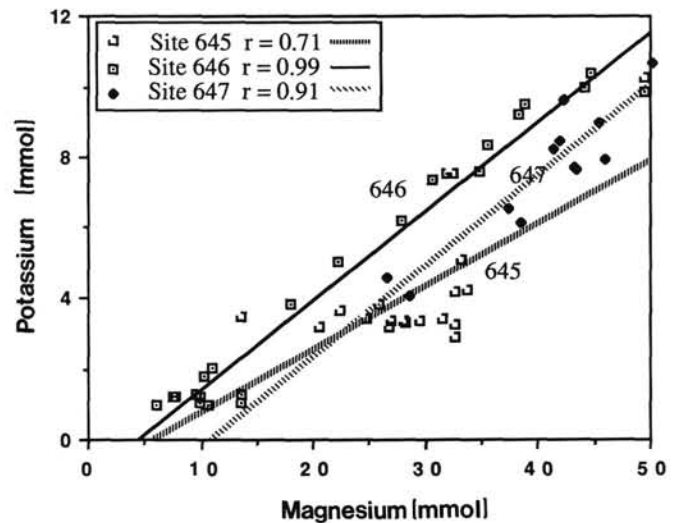


Figure 6. Plot of interstitial potassium vs. magnesium for each of the Leg 105 sites. Correlation coefficients are included.

The reaction products, H_2S and HCO_3 become involved in secondary reactions, ultimately leading to the authigenic precipitation of carbonate minerals, such as calcite and dolomite, and sulfides, such as pyrite. Pyrite is a common component of Units I and II sediments at Site 645 and makes up as much as 5% to 10% of the total sediment in portions of Unit II, usually in the form of encrustations and burrow fillings. Direct evidence for the formation of authigenic carbonate minerals is less obvious. Dolomite is abundant in the upper portions of Site 645, with a ratio of dolomite to calcite exceeding 2. Those few euhedral crystals detected by light microscope examination would indicate that some of this dolomite is authigenic; however, the presence of Cretaceous nannofossils and the high abundance of abraded rhombs would imply that much of the dolomite was deposited as glacial debris. A possible method to test for the origin of the various carbonate minerals would be through carbon isotope analyses. The authigenic carbonate that formed in the reducing pore-water system should be isotopically depleted relative to the surrounding biogenic carbonate (e.g., Lawrence et al., 1975). Indirect evidence for precipitation of authigenic carbonates comes from the HCO_3 , calcium, and magnesium concentration gradients at Site 645. Large decreases in total calcium and magnesium contents, the lowered alkalinity from 0 to 200 mbsf, and the close correspondence between ΔSO_4 and $\Delta\Sigma(\text{Ca} + \text{Mg})$ (Fig. 6) indicate that these ions are being sequestered into authigenic carbonates. The high ratio of $\Delta\text{Mg}/\Delta\text{Ca}$ implies that the primary authigenic carbonate may be dolomite. In deeper portions of Site 645, iron and manganese carbonate minerals, such as siderite and rhodochrosite, appear in trace quantities. The authigenesis of these minerals require that HS^- be low and dissolved manganese and iron be high (Garrels and Christ, 1965; von Rad and Botz, 1987).

Despite significant sulfate depletion with depth at Site 646, evidence of authigenic mineral formation is not as obvious. The calcium and magnesium gradients here depart only slightly from linear trends: calcium increases at a rate of 11.05 mmol/100 m, and magnesium decreases at a rate of 9.79 mmol/100 m over the upper 400 m. However, over the upper 150 m, where the rate of sulfate reduction is highest, calcium and magnesium, respectively, increase and decrease at rates of 1.68 and 15 mmol/100 m. The net change in $\Delta(\text{Ca} + \text{Mg})$ over this interval equals the decrease in the sulfate ion (Fig. 6), indicating that cations are being removed from the interstitial waters along with bicarbon-

ate ion. The low rate of increase with depth in the calcium content would indicate that a small amount of calcium is also being incorporated into the authigenic minerals.

Adsorption onto clay surfaces and/or incorporation into interlayers will also change cation concentrations. Drever (1974) demonstrated that under highly reducing conditions, magnesium substitutes for iron in the interlayer and/or on the surface of clay minerals. Potassium may also be removed by such processes. High concentrations of clay minerals, especially smectite, which has a high cation exchange capacity (H. Chamley, pers. comm., 1988), may allow for the uptake of magnesium as well as calcium through adsorption. As mentioned above, smectite is extremely abundant throughout Unit III at Site 645, and may lower overall calcium and magnesium contents slightly by absorption. In addition, authigenesis of clay minerals may occur if the HCO_3^- concentration is high enough and if an adequate source of SiO_2 and cations exists. A primary source for SiO_2 may be biogenic silica; opal-A is fairly unstable and will readily undergo transformation to opal-CT and, eventually, chert. Thus, in zones where active biogenic opal transformation is occurring, SiO_2 and cations may be used in the authigenesis of various clay minerals (Kastner and Gieskes, 1976). Under these conditions, additional magnesium may be removed in magnesium hydroxides (Kastner et al., 1977).

Oxygen and Hydrogen Isotopes

Of special interest are the concomitant decreases observed in deuterium and oxygen isotope compositions with depth at each site. The δD vs. $\delta^{18}\text{O}$ compositions of interstitial waters from the Leg 105 sites are plotted in Figure 7. At first glance, the downhole compositional variations of these isotopes may be linearly correlated at all three sites, implying similar controls on these gradients. However, closer inspection of the slopes of each regression reveals some variation from site to site. The difference in slope reflects inconsistencies in the oxygen isotope gradients. Sites 646 and 645 show similar magnitude gradients; however, more variability exists in the $\delta^{18}\text{O}$ curve from Site 645. In fact, as mentioned earlier, the oxygen isotope gradient actually reverses trend at lower intervals. This would indicate that several factors may ultimately contribute to the δD and $\delta^{18}\text{O}$ gradients in pelagic sequences. Similar trends in the isotopic composition

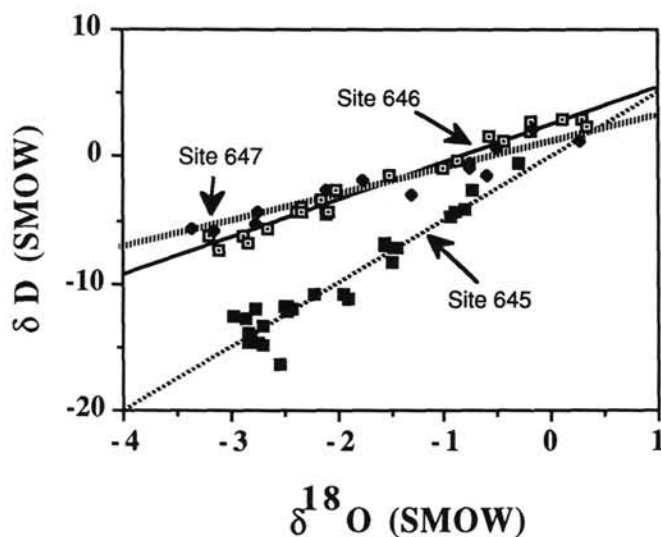


Figure 7. The interstitial-water δD vs. $\delta^{18}\text{O}$ compositions (SMOW) from Sites 645 (filled squares), 646 (open squares), and 647 (triangles).

of interstitial waters have been observed in globally distributed pelagic and hemipelagic sediments: their origin is still a topic of considerable debate. Several hypotheses have been proposed to explain these gradients:

1. One early hypothesis suggested that the observed oxygen and deuterium trends may be an artifact of squeezing. As waters filter through sediments, the clay component can act as a semi-permeable membrane that could preferentially absorb the heavier deuterium and oxygen isotopes, thus yielding progressively lighter expressed water (Coplen and Hanshaw, 1973). Such an effect could be enhanced by lower sediment porosities. However, the squeezing artifact as a source of the observed gradients can be immediately ruled out for several reasons. First, as Lawrence and Gieskes (1981) noted, some DSDP sites show no isotopic gradients at all or show a shift in one isotope but not the other. Second, there may be no systematic relationship between the isotopic compositions and the sediment porosities, amounts of water recovered, or pressures applied from actual Leg 105 shipboard sampling. Finally, in our own laboratory experiments, using sequential sampling during the squeezing process, we found no evidence of isotopic variation from initial composition, despite varying pressures and water/rock ratios.

2. If these trends are not an artifact of sampling, then the decreasing trend in $\delta^{18}\text{O}$ and deuterium must result from mixing by diffusion and/or advection of two isotopic end-members, the seawater above, and a light source below. The linear relationship between ΔCa and $\Delta\delta^{18}\text{O}$ that was observed at most DSDP sites has led several investigators to suggest that these gradients share a common origin, namely the low-temperature alteration to smectites of basalts and/or sedimentary volcanic material (Lawrence et al., 1975, 1979; Perry et al., 1976; Lawrence and Gieskes, 1981). Investigations of ophiolite sequences show that smectite alteration products are isotopically enriched in ^{18}O relative to the source material (Bohlke et al., 1981; Elthon et al., 1984), indicating that during alteration, ^{18}O isotopes are preferentially extracted from seawater into the smectites; however, the net effect of such a reaction on deuterium is uncertain. The average fractionation of deuterium between most primary tholeiite and alkali basalts and their glassy high- and low-temperature alteration products ranges from -100 to -40‰ (Kyser and O'Neil, 1984). Deuterium concentration in smectites, the primary alteration product of basalt, is uncertain. Savin and Epstein (1970) recorded values in the range of -100 to -40‰ for smectites in pelagic sediments. The average composition of basalts is nearer the depleted end of the range. Kyser and O'Neil (1984) estimated that the hydroxyl groups acquired during the low-temperature hydration of basalts are depleted in deuterium in the range of -100 to -80‰ , indicating that such reactions may, if anything, lead to a small enrichment in interstitial waters.

3. A further possibility is that the gradients result from the slow diffusion of isotopically lighter pre-glacial water stored within layers I or II (Lawrence and Gieskes, 1981; Friedman, 1987). Shackleton and Kennett (1975) estimated that the shift in the oxygen isotopic composition of the oceans resulting from continental glaciation is about 1.20‰ . This would translate into a value of 10‰ for deuterium. This could account for the magnitude of the shifts observed. The problem then becomes one of diffusion and mass balance. Assuming that the isotopic composition of the ocean has increased over time, at locations where sedimentation rates are low the rate of diffusion should have maintained pace with the upward migration of the sediment/water interface and would thus dissipate any expected gradients. However, at higher sedimentation rates, steady state would not be attained, and a gradient should develop, reflecting the change

in composition over time. All three of the Leg 105 sites are characterized by sedimentation rates that should be theoretically high enough to prevent such an isotopic gradient from being dissipated by diffusion processes alone.

Lawrence and Gieskes (1981) suggested that this large pool of paleowater could lie within layer II, if advective cycling occurred to great depths (1 km), with transport to layer I remaining diffusive. They maintained that this would also allow for the alteration of sufficient quantities of basalt to account for the observed ^{18}O depletions. Taking into account sedimentation rates and assuming a similar rate of diffusion at each site, one would expect the largest shift in values to be found at the site having the highest rates of sedimentation, that is, Site 645. For δD , the overall shift here is about -15‰ , compared with -10‰ for Site 646 and -8‰ for Site 647. Furthermore, a paleowater source might explain the more than 4‰ average difference between the Site 645 deuterium compositions and those from Sites 646 and 647. Compared to the Labrador Sea, the semi-enclosed Baffin Bay has probably received larger quantities of isotopically lighter glacial meltwater from the adjacent land masses. Although this hypothesis might help to explain the observed deuterium gradients, it cannot account for the differences in the $\delta^{18}\text{O}$ trend recorded at these sites, suggesting that the oxygen isotopic gradients may be altered by post-burial chemical reactions that do not affect deuterium equally.

Diagenetic reactions alone cannot be used to explain the observed isotopic gradients. However, they are capable of modifying the gradients in either a positive or negative direction. Lawrence (1973) and Lawrence et al. (1975) demonstrated that the conversion of biogenic silica to chert or of fossil carbonate to authigenic carbonate could decrease or increase the $\delta^{18}\text{O}$ of the pore waters, depending on the relative percentage and the starting isotopic compositions of each component, and the temperature at which the reactions take place. Increasing temperatures beyond 15°C , while keeping all other parameters constant, would have the effect of enriching interstitial waters. The oxygen isotope gradients display more nonlinearity with depth than deuterium. Below 450 mbsf at Site 645, $\delta^{18}\text{O}$ values show a gradual enrichment of 0.4‰ , while over the same interval δD values continue to decrease, indicating that diagenetic reactions involving either biogenic carbonate or silica or possibly even clay minerals are enriching pore waters in ^{18}O . Unfortunately, sediment isotopic data were not available for Site 645 at the time of this writing. However, bulk carbonate and planktonic and benthic foraminiferal isotopic data are available for Site 647 (Arthur et al., this volume) and suggest that substantial post-burial carbonate recrystallization occurred. Bulk carbonate and benthic foraminiferal $\delta^{18}\text{O}$ values become depleted by as much as 4‰ from 300 mbsf to the base of the hole. Incorporating porosity, heat flow, and pore-water $\delta^{18}\text{O}$ values into a simple mass-balance model, Arthur et al. (this volume) demonstrate that the changes recorded in sediment oxygen isotope values may have resulted from dissolution and recrystallization of only a small percentage of carbonate ($<25\text{‰}$) at depths below 300 mbsf. The net effect of such reactions on pore-water $\delta^{18}\text{O}$ may vary, depending on the rates of diffusion and thermal gradient; nonetheless, such reactions usually result in an overall enrichment.

SUMMARY

The concentration depth profiles at each of these sites are a function of a number of factors:

1. The general direction of the downhole gradients of the major and minor ions, including calcium, magnesium, potassium, lithium, and to a lesser extent, strontium result from the diffusion of ions between bottom waters above and the oceanic

crust below. The likely mechanism that changes the interstitial-water ion concentrations in the crust is the low-temperature alteration of basalt. Magnesium and potassium are effectively incorporated into basalts, while calcium and lithium are leached from these basalts.

2. Superimposed on these primary gradients are secondary anomalies that result from sedimentary reactions. The major driving force for these reactions comes from the reduction of sulfate ion, which in turn produces bicarbonate ion, a principal reactant in carbonate precipitation reactions. The effects of sulfate reduction are most evident at Site 645, where rapid depletions in both calcium and magnesium ions occur in the upper portion of the sections, mainly as a result of the precipitation of carbonate-bearing minerals, such as dolomite and/or calcite. Such depletions also occur at Site 646, but to a lesser extent.

3. Interstitial-water deuterium and oxygen isotope abundances must have originally reflected the composition of the bottom waters upon the time of burial. However, the inconsistent downhole slopes in the oxygen isotope gradients indicate that the original values may have been subsequently modified by chemical reactions involving layer II basalts and/or sediments. Deuterium does not appear to be similarly affected, although at the time of this writing, insufficient experimental data were available concerning the fractionation of hydrogen during low-temperature alteration of basalts to make a definitive statement.

ACKNOWLEDGMENTS

We thank three anonymous reviewers for their comments about this manuscript and D. Cullen for technical support.

REFERENCES

- Bohlke, J. K., Honnorez, J., Honnorez-Guerstein, B.-M., Muehlenbachs, K., and Peterson, N., 1981. Heterogeneous alteration of the upper oceanic crust: Correlation of rock chemistry in basalts from Site 396B, DSDP. *J. Geophys. Res.*, 86:7935-7950.
- Coplen, T. B., and Hanshaw, B. B., 1973. Ultrafiltration by a compacted clay membrane, oxygen and hydrogen isotopic fractionation. *Geochim. Cosmochim. Acta*, 37:2295-2310.
- Craig, H., 1961. Isotopic variations in meteoric waters. *Science*, 135:1702.
- Drever, J. I., 1974. The magnesium problem. In Goldberg, D. (Ed.), *The Sea*, 5:337-358.
- Elthon, D., Lawrence, J. R., Hanson, R. E., and Stern, C., 1984. Modeling of oxygen isotope data from the Sarmiento ophiolite complex, Chile. In Gass, I. G., Leppard, S. J., and Shelton, A. W. (Eds.), *Ophiolites and Oceanic Lithosphere*. Geol. Soc. Am. Spec. Publ., 13:185.
- Emerson, S., 1985. Organic carbon preservation in marine sediments. In Sundquist, E. T., and Broecker, W. S. (Eds.), *The Carbon Cycle and Atmospheric CO₂. Natural Variations Archean to Present*. Geophys. Soc. Am. Mono., 32:78-88.
- Epstein, S., and Mayeda, T., 1953. Variations in ^{18}O content of waters from natural sources. *Geochim. Cosmochim. Acta*, 27:213-224.
- Fanning, K. A., and Pilson, M.E.Q., 1973. On the spectrophotometric determination of dissolved silica in natural waters. *Anal. Chem.*, 45:136-140.
- Friedman, I., 1953. Deuterium content of natural waters. *Geochim. Cosmochim. Acta*, 4:89.
- _____, 1987. Deuterium in interstitial water from deep-sea cores. *Trans., Am. Geophys. Un.*, 86(16):469 (Abstract).
- Garrels, R. M., and Christ, C. L., 1965. *Solutions, Minerals and Equilibrium*: New York (Harper).
- Gieskes, J. M., 1974. Interstitial water studies, Leg 25. In Simpson, E.S.W., Schlich, R., et al., *Init. Repts. DSDP*, 25: Washington (U.S. Govt. Printing Office), 361-394.
- _____, 1981. Deep-sea drilling interstitial water studies: implication for chemical alteration of the oceanic crust, layers I and II. *Soc. Econ. Paleontol. Mineral. Spec. Publ.*, 32:149-167.
- _____, 1983. The chemistry of interstitial waters of deep-sea sediments: interpretation of deep-sea drilling data. In Riley, J. P. (Ed.), *Chemical Oceanography*, 8:222-271.

- Gieskes, J. M., Elderfield, H., and Palmer, M. R., 1986. Strontium and its isotopic composition in interstitial water of marine carbonate sediments. *Earth Planet. Sci. Lett.*, 77:229-235.
- Kastner, M., Keene, J. B., and Gieskes, J. M., 1977. Diagenesis of siliceous oozes—I. chemical controls on the rate of opal-A to opal-CT transformation: an experimental study. *Geochim. Cosmochim. Acta*, 41:1041-1059.
- Kyser, T. K., and O'Neil, J. R., 1984. Hydrogen isotope systematics of submarine basalts. *Geochim. Cosmochim. Acta*, 48:2123-2130.
- Lambert, C. E., and Oviatt, C. A., 1986. *Manual of Biological and Geochemical Techniques in Coastal Areas*: Kingston, RI (Univ. of Rhode Island), MERL Ser. Rept. 7, 2nd ed.
- Lawrence, J. R., 1973. Interstitial water studies, Leg 15—Stable oxygen and carbon isotope variation in water, carbonate, and silicates from the Venezuela Basin (Site 149) and the Aves Rise (Site 148). In Heezen, B. C., MacGregor, I. D., et al., *Init. Repts. DSDP*, 20: Washington (U.S. Govt. Printing Office), 891-899.
- Lawrence, J. R., Drever, J. I., Anderson, T. F., Brueckner, H. K., 1979. Importance of alteration of volcanic matter in the sediments of Deep Sea Drilling Site 323: Chemistry $^{18}\text{O}/^{16}\text{O}$ and $^{87}\text{Sr}/^{86}\text{Sr}$. *Geochim. Cosmochim. Acta*, 43:573-588.
- Lawrence, J. R., and Gieskes, J. M., 1981. Constraints on water transport and alteration in the oceanic crust from isotopic composition of pore water. *J. Geophys. Res.*, 86:7924-7934.
- Lawrence, J. R., Gieskes, J. M., and Broecker, W. S., 1975. Oxygen isotope and cation composition of DSDP pore waters and the alteration of layer II basalts. *Earth Planet. Sci. Lett.*, 27:1-11.
- Manheim, F. T., and Sayles, F. L., 1974. Composition and origin of interstitial waters of marine sediments based on deep-sea drill cores. In Goldberg, E. D. (Ed.), *The Sea*, Vol. 5: New York (Wiley-Interscience), 527-568.
- McDuff, R. E., 1981. Major cation gradients in DSDP interstitial waters: the role of diffusive exchange between seawater and upper oceanic crust. *Geochim. Cosmochim. Acta*, 45:1705-1713.
- McDuff, R. E., and Gieskes, J. M., 1976. Calcium and magnesium profiles in DSDP interstitial waters: diffusion or reaction? *Earth Planet. Sci. Lett.*, 33:1-10.
- Perry, E. A., Gieskes, J. M., and Lawrence, J. R., 1976. Mg, Ca, and $^{18}\text{O}/^{16}\text{O}$ exchange in sediment pore-water system, Hole 149, DSDP. *Geochim. Cosmochim. Acta*, 40:413-423.
- Savin, S. M., and Epstein, S., 1970. The oxygen and hydrogen isotopic geochemistry of ocean sediments and shales. *Geochim. Cosmochim. Acta*, 34:43-63.
- Seyfried, W. E., and Bischoff, J. L., 1979. Low-temperature basalt alteration by seawater: an experimental study at 70° and 15°C. *Geochim. Cosmochim. Acta*, 43:1937-1947.
- Seyfried, W. E., Jr., Janecky, D. R., and Mottl, M. J., 1984. Alteration of the oceanic crust: implications for geochemical cycles of lithium and boron. *Geochim. Cosmochim. Acta*, 48:557-569.
- Shackleton, N. J., and Kennett, J. P., 1975. Paleotemperature history of the Cenozoic and the initiation of Antarctic glaciation: oxygen and carbon isotope analyses in DSDP Sites 277, 279, and 281. In Kennett, J. P., Houtz, R. E., et al., *Init. Repts. DSDP*, 29: Washington (U.S. Govt. Printing Office), 743-754.
- von Rad, U., and Botz, R., 1987. Authigenic Fe-Mn carbonates in Cretaceous and Tertiary sediments of the continental rise of eastern North America, Deep Sea Drilling Project Site 603. In van Hinte, J. E., Wise, S. W., Jr., et al., *Init. Repts. DSDP*, 93: Washington (U.S. Govt. Printing Office), 1061-1077.

Date of initial receipt: 29 July 1987

Date of acceptance: 3 February 1989

Ms 105B-161